S©MR

СИБИРСКИЕ ЭЛЕКТРОННЫЕ
МАТЕМАТИЧЕСКИЕ ИЗВЕСТИЯ
Siberian Electronic Mathematical Reports
http://semr.math.nsc.ru
ISSN 1813-3304

Vol. 23, No. 1, pp. 532–553 (2026) УДК 519.61
https://doi.org/10.33048/semi.2026.23.032 MSC 65F99

CONSTRUCTION AND ESTIMATION OF STABLE SOLUTIONS OF CAUCHY PROBLEMS INCREASING ON THE INITIAL TIME INTERVAL

E.A. BIBERDORF, L. WANG

Communicated by M.I. Protasov

Abstract: Two algorithms are presented that allow one to find initial data for asymptotically stable solutions to Cauchy problems for ODE systems that are increasing over the initial time interval. One algorithm uses eigenvectors, while the other is based on the matrix spectrum dichotomy method. Using these algorithms, locally increasing solutions were constructed for the flutter models and the Navier-Stokes system linearized in the neighborhood of plane-parallel Poiseuille flow. A two-sided estimate for the maximum norm of these solutions was obtained.

Keywords: Cauchy problem, stability, spectral criterion, matrix spectrum dichotomy.

1 Introduction

One of the most common mathematical methods of studying stability is the spectral approach. It is based on the linearization of the differential operator describing the process under study, with respect to small perturbations. Next, the presence or absence of points in the spectrum of the

---

Biberdorf E.A., Wang L. Construction and estimation of stable solutions of Cauchy problems increasing on the initial time interval.

This work was accomplished within the state assignment of the Institute of Mathematics, Siberian Branch of the Russian Academy of Sciences, project no. FWNF-2026-0028.

Received January, 14, 2026, Published June, 3, 2026.

linearized operator, which are responsible for the growth of the perturbations, is determined in the corresponding instability region on the complex plane. Experimental data indicate that physical processes modeled by solutions of initial-boundary value problems can exhibit instability even when all eigenvalues of the linearized operator lie in the stability region. This phenomenon is observed, in particular, during subcritical laminar-turbulent transitions in viscous incompressible fluid flows (see references in [2]). It has been suggested that such «practical» instability is related to the fact that even in the case of spectral asymptotic stability, the linearized problem can have solutions that exhibit significant growth in the initial time interval. As an example of a paper investigating this mechanism of transient growth of disturbances in stable fluid flows, we can cite the article [2]. The main idea implemented in the article is an orthogonal decomposition of the solution space into two subspaces, with growing solutions represented as the sum of two nonzero terms belonging to one and the other subspace.

In this paper, we conduct a comprehensive study of locally increasing solutions of the Cauchy problem $dy/dt = Ay,\ y|_{t=0} = y_0$ under the condition that the spectral criterion for asymptotic stability is satisfied. Below, we present two algorithms for finding such solutions and examples of their application. We also obtain estimates for the maximum of their norm (see section 4), among which the lower bound is of particular importance.

The first algorithm (see section 2) is based on analogies with the behavior of solutions of the Cauchy problem when the matrix has Jordan blocks. To calculate the initial data of the growing solution, this approach requires knowledge of the eigenvectors.

The second algorithm (see section 3) is conceptually similar to the approach described in the aforementioned work [1], but differs from it in its much more general nature and broader potential range of application. The new method also involves decomposing the solution space into subspaces, for which the initial data space is first decomposed. The matrix spectrum dichotomy method (see [3]-[15]) is used as a tool for this decomposition.

The problem of dichotomy of the spectrum of a matrix pencil $A - \lambda B$ with respect to a curve γ involves computing the matrix $H = H^* > 0$, whose norm serves as a numerical criterion for the feasibility of separating the eigenvalues of the pencil $A - \lambda B$ by the curve γ. In particular, it can be used to estimate the distance from the spectrum to the curve. Projection matrices $P^2 = P$ onto the reducing subspaces of the pencil corresponding to the parts of the spectrum lying on opposite sides of γ are also computed, while the bases of the reducing subspaces are determined using singular value decompositions of the projectors. If γ is a circle, then the algorithm for dichotomy of the spectrum with respect to it is an iterative process, with the main action at each iteration being the qr decomposition. The imaginary-axis dichotomy algorithm is the unit-circle dichotomy algorithm applied to a matrix exponential or a fractional-linear transformation. In Section 4 of

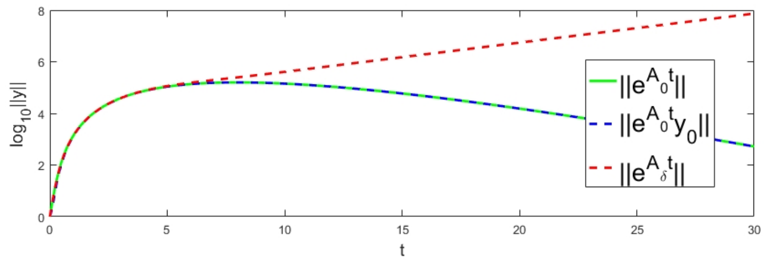

FIG. 1. Solution of the Cauchy problem corresponding to the matrices A_0 and A_δ, $\delta = 5 \cdot 10^{-6}$

this paper, we formulate new properties of the line dichotomy and use them to obtain estimates for growing solutions of the Cauchy problem.

2 Eigenvector method

2.1. Preliminary remarks. As an example, let us consider the system $y' = A_\delta y$, the matrix of which at $\delta = 0$ is a Jordan cell of size 5×5, in which all eigenvalues are located in the left half-plane:

$$A_\delta = \begin{bmatrix} -0.5 & 15 & & & \\ & -0.5 & 15 & & \\ & & -0.5 & 15 & \\ & & & -0.5 & 15 \\ \delta & & & & -0.5 \end{bmatrix}.$$

With a small perturbation of $\delta = 5 \cdot 10^{-6}$, the Jordan structure is destroyed, and the matrix A_δ also acquires an eigenvalue in the right half-plane. This means that a small perturbation transforms asymptotic stability into instability. Fig. 1 shows an obvious situation where the norm of the exponent of the stable matrix A_0 tends to zero, while the exponent of the perturbed matrix A_δ grows infinitely (here and below, unless otherwise stated, the spectral norm is used for matrices, and the Euclidean norm is used for vectors). However, in addition to this, on the initial interval of the variable t, the matrix exponent $e^{A_0 t}$ also exhibits rapid growth. In this case, this is easily explained by the fact that the matrix exponent of a Jordan cell such as A_0 has elements of the form $t^k e^{\lambda t}$. The largest contribution to the growth of the norm comes from the element in the last column of the first row, which contains the maximum power of the parameter t.

Let us turn to the question of choosing the initial data for the solution of the Cauchy problem, growing over the initial time interval. It is easy to establish that by choosing the last adjoint vector in the Jordan chain $y_0 = [0, 0, 0, 0, 1]^T$, we obtain maximum growth, and the same amplification mechanism will be activated as for the matrix exponential. The graphs of the norms of this solution and the matrix exponential coincide (Fig. 1). Generally speaking, if the system matrix contains a Jordan block, then a growing solution can be obtained by taking the last adjoint vector as the initial data.

However, due to the density of the set of diagonalizable matrices in the matrix space, when using a computer for calculations, it is possible to obtain only a few very close eigenvectors for the matrix A_0:

$$v_1 = [1, 0, 0, 0, 0]^T, \ \ v_2 = [-1, 10^{-18}, 0, 0, 0]^T, \ \ v_3 = [1, -10^{-18}, 10^{-35}, 0, 0]^T,$$

$$v_4 = [-1, 10^{-18}, -10^{-35}, 10^{-52}, 0]^T, \ \ v_5 = [1, -10^{-18}, 10^{-35}, -10^{-52}, 10^{-69}]^T.$$

Nevertheless, the previously selected vector $y_0 = [0, 0, 0, 0, 1]^T$ yields the same growing solution. Note that in this case, the vector y_0 differs in that it is orthogonal to four of the five eigenvectors and orthogonal to the fifth with high accuracy. Based on this observation, as the initial data, we will choose a vector that forms, in some sense, the maximum angle with all eigenvectors.

2.2. Angles between vectors. Let $v_1, \dots, v_k$ be some group of normalized linearly independent vectors from an n-dimensional space, $k \le n$, $\|v_j\| = 1$, and let the normalized vector y_0 be their linear combination: $y_0 = Va$, where $V = [v_1, \cdots v_k]$, $a = [a_1, \dots, a_k]^T$, $\|y_0\| = 1$ (see the diagram in Fig. 2, left). The following definition is quite natural.

Definition 1. If α_j is the angle between vectors y_0 and v_j, then the angle between y_0 and the set of vectors $v_1, \dots, v_k$ will be called $\alpha = \min_j \alpha_j$.

Obviously, this angle satisfies an equality that completely defines it.

$$|\cos\alpha| = \max_j |\cos\alpha_j| = \max_j |(v_j, y_0)| = \|V^* y_0\|_\infty, \tag{1}$$

where $(\cdot,\cdot)$ is the scalar product.

Based on the representation (1), the angle between y_0 and the set $\{v_j\}$ can be determined in a different way, using not the minimum, but, in a certain sense, the average value of the angles α_j.

Definition 2. The angle between y_0 and $\{v_j\}$ in the sense of the mean value is the value α for which the relation is satisfied

$$|\cos\alpha| = \frac{1}{k}\sqrt{\sum_{j=1}^{k} |\cos\alpha_j|^2} = \frac{1}{k}\sqrt{\sum_{j=1}^{k} |(v_j, y_0)|^2} = \frac{1}{k}\|V^* y_0\|. \tag{2}$$

In this case, the sign $\|\cdot\|$ denotes the Euclidean norm.

Now let us turn to the problem of choosing y_0 that forms the maximum angle with the set $\{v_j\}$, that is, minimizes the value $\|V^* y_0\|$. Consider the spectral (also known as singular) decomposition $V^*V = W\Lambda W^*$, where the diagonal elements of the matrix Λ are positive, nonzero, and arranged in descending order $\lambda_1 \ge \lambda_2 \ge \cdots \ge \lambda_k$. Let w_j be the columns of the matrix W. Using this notation, we formulate and prove the lemma, which is the theoretical basis of the first algorithm.

Lemma 1. *The vector $y_0 = V \cdot w_k$ forms the maximum possible angle in the sense of Definition 2 with the vectors $v_1, \dots, v_k$.*

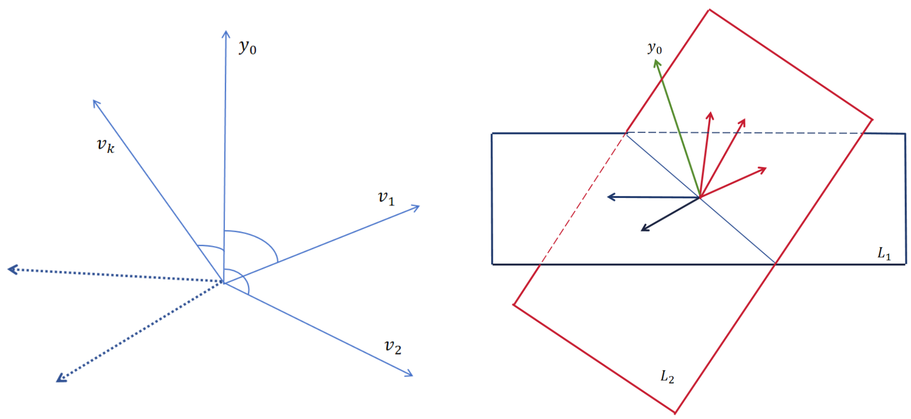

FIG. 2. Scheme for algorithm 1 (left), for algorithm 2 (right)

Proof. Let y be an arbitrary normalized vector belonging to the linear span of vectors $\{v_j\}$: $y = Vc$, where $c = [c_1, ..., c_k]^T$. Note that since y and v_j are normalized, it follows that $\|c\| = 1$. Consider the norm of the product

$$\|V^*y\| = \|W\Lambda W^*c\| = \|\Lambda W^*c\| = \|\Lambda\tilde{c}\|,$$

where $c = W\tilde{c}$. It is obvious that $\min_{\tilde{c}} \|\Lambda\tilde{c}\| = \lambda_k$ and is achieved when $\tilde{c} = [0, \ldots, 0, 1]^T$, that is, when $y = y_0 = V \cdot w_k$, which is what was required to be proven. This result leads to the following algorithm.

Algorithm 1
Given: matrix A.
Step 1. Calculate the matrix V consisting of the eigenvectors of matrix A.
Step 2. Find a factorization for matrix $S = V^*V$ such that $S = W\Lambda W^*$, where $W = \begin{bmatrix} w_1 & w_2 & \cdots & w_k \end{bmatrix}$ is an orthogonal matrix, $\Lambda = \operatorname{diag}(\lambda_1, \ldots, \lambda_k)$, $\lambda_j > 0$ are arranged in descending order.
Step 3. $y_0 = V \cdot w_k$

2.3. Example: Wing flutter model. Let's consider one of the mathematical models of wing flutter described in [11]. It is a system of ordinary differential equations, where the system matrix is expressed as follows

$$A = \begin{bmatrix} -vD & -(G + v^2F) \\ I & 0 \end{bmatrix}, \qquad G = \begin{bmatrix} 37.7 & & & \\ & 169 & & \\ & & 899 & \\ & & & 1792 \end{bmatrix},$$
$$D = 0.73 \cdot 10^{-2} I, \qquad F = 10^{-3} \begin{bmatrix} 0 & -1.97 & 0 & 0 \\ 0.12 & 0 & -4.19 & 0.171 \\ 0 & 0.176 & 0 & 0 \\ 0 & -0.154 & 0 & 0 \end{bmatrix}. \qquad (3)$$

Here v is the flow velocity, G is the matrix of natural oscillation frequencies, vD is the friction matrix, v^2F is the matrix of interactions between the wing parts, and y is the displacement vector. For the numerical experiment, we use the value $v = 425$, which is below the critical value, i.e., all eigenvalues of the matrix (3) lie in the left half-plane:

$$\lambda_{1,2} = -3.0922 \pm i10.9845, \quad \lambda_{3,4} = -0.0103 \pm i10.9845,$$

$$\lambda_{5,6} = -1.5513 \pm i29.3672, \quad \lambda_{7,8} = -1.5512 \pm i42.2974.$$

To select the initial data for the Cauchy problem, we use Algorithm 1. To do this, we first apply it to the group of eigenvectors v_1, v_2, v_3, v_4 corresponding to the eigenvalues $\lambda_1, \dots, \lambda_4$, and then to all eigenvectors $v_1, \dots, v_8$. The norms of the resulting solutions are shown in Fig. 3. Both solutions exhibit growth in the initial period of time.

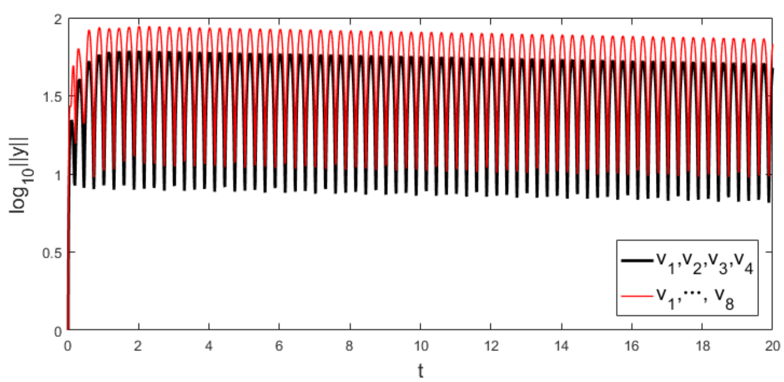

FIG. 3. Solution of the Cauchy problem for the flutter model system at $v = 425$.

3 Method of invariant subspaces

3.1. Brief description of the method. Recall that the asymmetric spectral problem in the classical formulation can be very sensitive to errors when calculating both eigenvalues and eigenvectors. In contrast, the matrix spectrum dichotomy problem offers several advantages. One of these is the algorithm's ability to «self-diagnose», meaning that the computational robustness of the obtained result is determined simultaneously during its execution. For this reason, this method is preferable for a large number of problems. The basic idea of the method for choosing initial values for solutions of the Cauchy problem growing over a finite interval remains the same: we must determine y_0 that forms the largest possible angle with the eigenvectors. However, in this case, we generalize the concept of eigenvectors to invariant subspaces of a matrix. Therefore, to obtain y_0, we must partition the initial data space into invariant subspaces. The simplest case is a partition into two subspaces, which is accomplished using the dichotomy method.

We choose a line that divides the set of eigenvalues into two parts, one of which contains the critical value (i.e., the one closest to the imaginary axis). We apply the matrix pencil dichotomy method with respect to this line, resulting in bases of invariant subspaces corresponding to the separated groups of eigenvalues. Next, we choose the initial vector y_0 such that the angle between it and the bases of both subspaces is maximal (see the diagram in Fig. 2 on the right), using Definition 2 and Lemma 1.

Algorithm 2
Given: matrix A, line γ
Step 1. Using dichotomy, calculate the projectors P_1, P_2 onto the invariant subspaces of matrix A corresponding to the eigenvalues lying on opposite sides of γ.
Step 2. Calculate the singular value decompositions of the projectors $P_j = U_j S_j V_j^*$
Step 3. From the first k_1 and k_2 columns of matrices U_1 and U_2, form a matrix

$$V = [U_1(:, 1 : k_1), U_2(:, 1 : k_2)]\,, \text{ where } k_j = \mathrm{tr} P_j.$$

Step 4. Find a factorization for the matrix $S = V^*V$ such that $S = W\Lambda W^*$, where $W = \begin{bmatrix} w_1 & w_2 & \cdots & w_n \end{bmatrix}$ is an orthogonal matrix, $\Lambda = \mathrm{diag}(\lambda_1, \ldots, \lambda_n)$, $\lambda_j > 0$ are arranged in descending order.
Step 5. $y_0 = V \cdot w_n$

3.2. Examples.

3.2.1. Wing flutter model. Let us apply Algorithm 2 to the flutter model (3) considered earlier. We use the dichotomy of the spectrum with respect to the following lines: the real axis (highlighted in red and denoted by the number 1 in Fig. 4), the line $Im\ \omega = 12$ (blue, number 2), the line $Re\ \omega = -1$ (green, number 3), the line $Im\ \omega = 3Re\,\omega + 15$ (black, 4). As a result, four variants of the initial conditions for the Cauchy problem are obtained, presented in Table 1. These initial data correspond to solutions of the Cauchy problem, the Euclidean norm of which for each t is shown in Fig. 5. In all four cases, despite the significantly different initial conditions, the solution has a maximum. Moreover, when using straight lines 3 and 4, the

TABLE 1. Initial values for the flutter model (3)

$10^{-4} \cdot y_0$	line 1	line 2	line 3	line 4
y_0^1	0	-62-3i	-19	123-96i
y_0^2	-i	161+8i	-87	563-196i
y_0^3	-i	203-7i	-46	551-169i
y_0^4	1-9i	-3+i	1	-10+3i
y_0^5	4-30i	1-10i	-1690	-5-1545i
y_0^6	-15+100i	24-470i	-7095	-2318-6003i
y_0^7	-40+265i	522-9920i	-6840	-565-7425i
y_0^8	1476-9886i	-53+1016i	131	6+200i

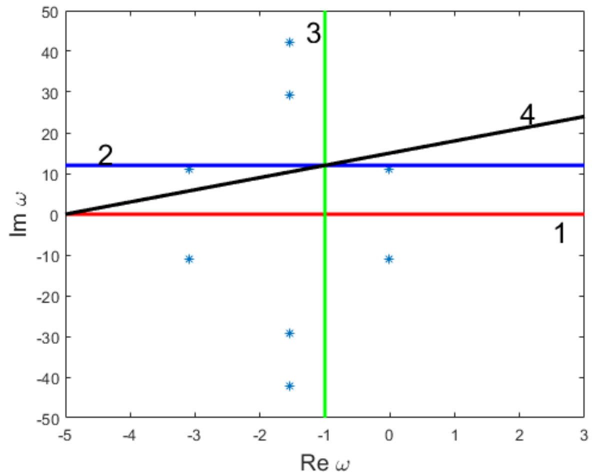

FIG. 4. The spectrum of the matrix (3) at $v = 425$ and the lines used in the example dividing it into parts

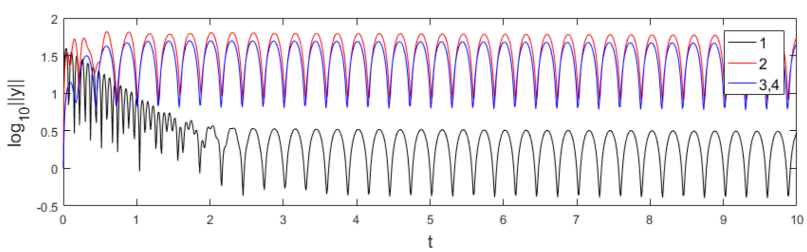

FIG. 5. Solution of the Cauchy problem with matrix (3), lines are used for separation see fig.4

solution is real-valued in one case and complex-valued in the other, with both solutions increasing by almost two orders of magnitude.

3.2.2. Infinite strip panel flutter model. We will examine the model previously discussed in works [14],[16]. The dimensionless equation for the perturbed state $u(t, x, y)$ of an infinite plate has the form

$$M\Delta^2 u + \gamma\vec{v}\nabla u + \gamma\frac{\partial u}{\partial t} + \rho h\frac{\partial^2 u}{\partial t^2} = 0.$$

Here $\vec{v}$ is the free-stream velocity, Δ^2 is the biharmonic operator, γ is the gas specific heat index, E is Young's modulus, h is the constant plate thickness, ν is Poisson's ratio, ρ is the material density, and $M = Eh^3/(12(1-\nu^2))$ is a constant.

Different methods of fastening the strip edges at $y = 0$ and $y = 1$ are described by the corresponding boundary conditions. For hinged and rigid edge fastening, they are:

$$u = 0, \frac{\partial^2 u}{\partial y^2} = 0 \;\text{ and }\; u = 0, \frac{\partial u}{\partial y} = 0$$

respectively.

Substituting a solution of the form $u(t, x, y) = \varphi(t, y)e^{-i\alpha x}$ into the equation and boundary conditions leads to an initial-boundary value problem with one spatial variable for each fixed α. For finite-dimensional approximation of the boundary value and spectral problems, it is necessary to discretize the differential operators taking into account the boundary conditions. For this purpose, matrices of collocation derivatives are used, the choice of which is described in more detail in the paper [14]. We only note that for the case of hinged fastening, the matrices described in the paper [17] are suitable, and for rigid fastening, those in the paper [18]. As a result, we obtain the Cauchy problem for a system of second-order ordinary differential equations

$$\rho h \frac{d^2\varphi}{dt^2} + \gamma \frac{d\varphi}{dt} + C\varphi = 0,$$

where

$$C = M[D_N^4 - 2\alpha^2 D_N^2 + \alpha^4 I_N] + \gamma v_y D_N - i\alpha\gamma v_x I_N,$$

D_N is the collocation matrix derivative, I_N is the identity matrix. Using the standard transition to a new unknown vector function, we obtain a first-order ODE system, but twice as large:

$$B\frac{d}{dt}\psi = A\psi, \text{ where } A = \begin{bmatrix} C & \gamma I \\ 0 & I \end{bmatrix}, \quad B = \begin{bmatrix} 0 & \rho h I \\ I & 0 \end{bmatrix}, \quad \psi = \begin{pmatrix} \varphi \\ \frac{d}{dt}\varphi \end{pmatrix}, \tag{4}$$

We fix the value of the velocity vector components $v_x = 0.1606$, $v_y = 0$ for hinged fastening, $v_x = 0.0906$, $v_y = 0$ for rigid fastening and calculate the initial data for the Cauchy problem using Algorithm 2 with the following constant values:

$$\alpha = 1,\ \gamma = 1.4,\ E = 7 \cdot 10^5,\ h = 3 \cdot 10^{-3},\ \nu = 0.33,\ \rho = 2.7 \cdot 10^3,\ N = 30.$$

Note that the values of α and $\vec{v}$ are such that the entire spectrum of the pencil $A - \omega B$ is located strictly in the left half-plane.

In the case of hinged edge fixation, the first step of Algorithm 2 performs a spectrum dichotomy with respect to the following lines:

1. line $Re\,\omega = -0.08$ (see Fig. 6, top left, marked in red);
2. line $Re\,\omega = -0.02$ (Fig. 6, top left, black);
3. line $Im\,\omega = -1578 Re\,\omega - 134$ (Fig. 6, top left, blue).

When the strip edges are rigidly fixed, a spectrum division with respect to the lines is used:

1. line $Re\,\omega = -0.08$ (Fig. 6, top right, red);
2. line $Re\,\omega = -0.02$ (Fig. 6 top right, black);
3. line $Im\,\omega = 10$ (Fig. 6 top right, blue).

The dependence of the norm of solutions to the Cauchy problem (4) on t with initial data obtained using Algorithm 2 can be seen in the central and lower

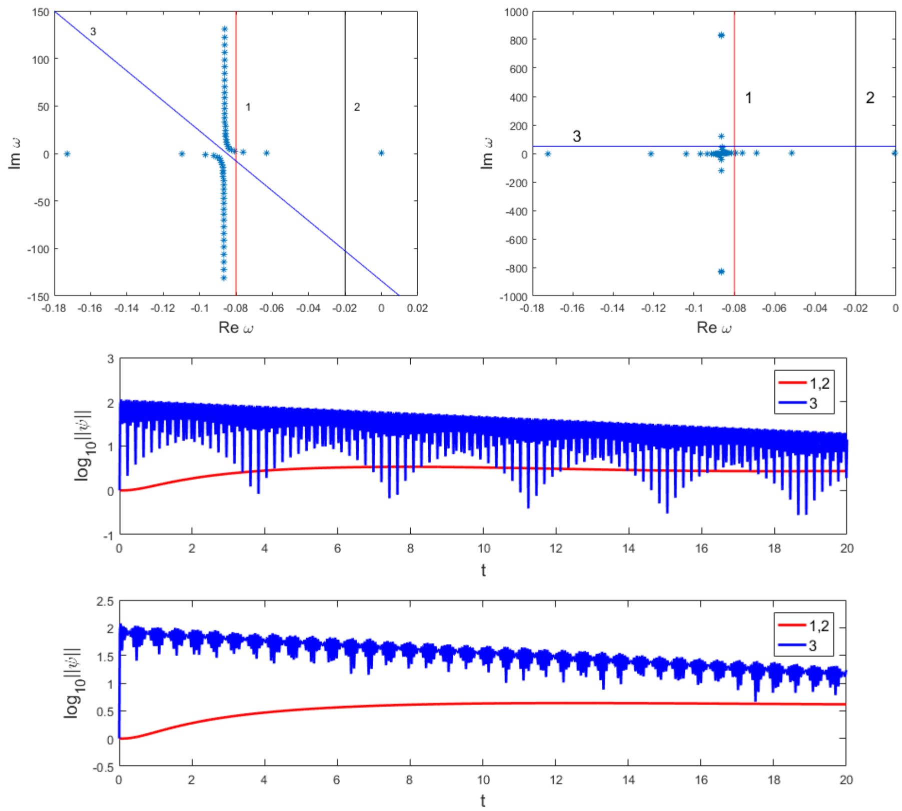

FIG. 6. Top: eigenvalues of the pencil $A - \omega B$ and the lines with respect to which the spectrum is divided (on the left, hinged fastening, on the right, rigid fastening); the norm of the solution of the Cauchy problem for the system (4) (in the center, hinged fastening, below, rigid fastening).

panels of Fig.6. For both the hinged and rigid fixations, using lines 1 and 2 (red) leads to a solution that exhibits a slight increase and an extremely slow decay. The latter is likely due to the critical eigenvalue being very close to the imaginary axis.

The use of line 3 (blue color) for dichotomy in both cases allows us to obtain solutions that sharply increase by two orders of magnitude, while the rate of subsequent decrease is just as small as in the cases of lines 1, 2.

3.2.3. Navier-Stokes system. By analogy with the derivation of the Orr-Sommerfeld equation, the linearization of the Navier-Stokes system of equations for a viscous incompressible fluid

$$\begin{cases} \dfrac{\partial U}{\partial t} + (U, \nabla)U = -\nabla P + \dfrac{1}{Re}\Delta U, \\ \operatorname{div} U = 0 \end{cases}$$

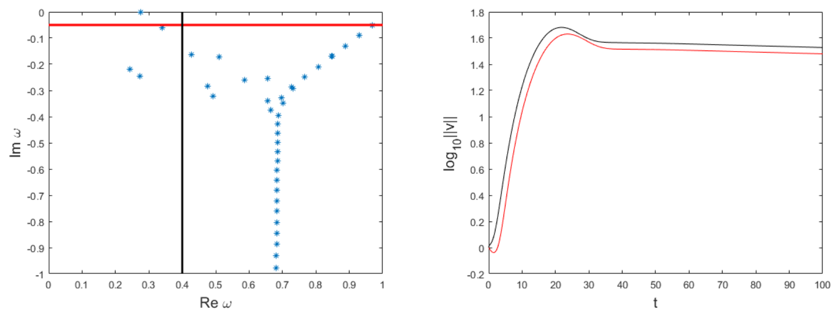

FIG. 7. Eigenvalues of the matrix pencil $A+i\omega B$ (6) and lines dividing the spectrum into parts (left), norms of solutions of the system (6) (right).

in the neighborhood of a plane-parallel Poiseuille flow $U = (1-y^2, 0, 0)^T$, $P = -2x/Re$ relatively small perturbations of the form $[u(t, y), v(t, y), w(t, y)]^T e^{i(\alpha x+\beta z)}$, $p(t, y)e^{i(\alpha x+\beta z)}$ and successive elimination of variables leads to a one-dimensional initial-boundary value problem for the function v :

$$iRe\left(\frac{\partial^2}{\partial y^2}-k^2\right)^2\frac{\partial}{\partial t}v = \\ = \left[\left(i\alpha Re(1-y^2)-1\right)\left(\frac{\partial^2}{\partial y^2}-k^2\right)^2+2i\alpha Re\right]v, \\ v|_{y=\pm1} = v_y|_{y=\pm1} = 0, \quad v|_{t=0} = v_0 \tag{5}$$

Here $-1 \le y \le 1$, Re is the Reynolds number, $\kappa^2 = \alpha^2 + \beta^2$. We use the collocation matrix derivatives D_N (see [18]) to discretize the derivatives with respect to the variable y (y_j are the collocation points), resulting in the Cauchy problem for the system of ordinary differential equations where

$$B\frac{d}{dt}v = Av, \text{ where} \\ A = \left(i\alpha Re\,\mathrm{diag}(1-y_j^2)-I\right)\left(D_N^2-k^2I\right)^2+2i\alpha Re\,I, \\ B = iRe\left(D_N^2-k^2I\right)^2. \tag{6}$$

For the numerical experiment, we use the parameter values $Re = 5000$, $\alpha = 1.02$, $\beta = 0$, for which the zero solution is asymptotically stable, and the number of collocation points $N = 100$. We obtain the initial vector v_0 using Algorithm 2. The dichotomy method is applied with respect to the following lines:

(1) line $Im\ \omega = -0.05$ (Fig. 7, red);
(2) line $Re\ \omega = 0.4$ (Fig. 7, black).

In Fig. 11, the left shows how these lines divide the spectrum of the matrix pencil $A+i\omega B$, and the right shows the norms of the solutions to the problem (5) for these two cases. It can be noted that both obtained solutions grow over the initial time interval, with the growth amounting to approximately two orders of magnitude.

4 A priori estimates of solutions of the Cauchy problem

For the maximum norm of the solution of the Cauchy problem for the system $y' = Ay$ there is a well-known estimate obtained by M.G. Krein [10], [19]:

$$\|y(t)\| \le \sqrt{\operatorname{cond}(H)}\, e^{-t/(2\|H\|)}\|y_0\|,$$

where cond is the condition number, and H is the solution of the Lyapunov equation

$$HA + A^* H = -I,$$

which can be represented in integral form

$$H = \frac{1}{2\pi}\int_{-\infty}^{+\infty} (A^* + i\xi I)^{-1} C (A - i\xi I)^{-1} d\xi, \;\; C = I,$$

and coincides with the matrix criterion for the dichotomy of the spectrum of the matrix A with respect to the imaginary axis. In practice, this estimate is usually quite high, but for a large value of $\operatorname{cond}(H)$ it is a warning that the solution may grow significantly over the initial time interval.

The following theorem also describes the conditions under which a solution to the Cauchy problem with a local maximum can exist. Note that the theorem provides not only an upper bound but also a lower bound.

Theorem 1. *Let the matrix A have its entire spectrum in the left half-plane. Let the angle between two fixed eigenvectors be α, and let the corresponding eigenvalues be $\lambda_j = \alpha_j + i\beta_j$, $j = 1, 2$, $\alpha_1 \le \alpha_2 < 0$. Then there exists a solution to the Cauchy problem $y' = Ay$, $y(0) = y_0$, $\|y_0\| = 1$, with a local maximum of the norm M such that*

$$\begin{aligned} &\operatorname{ctg}\alpha \frac{\alpha_2 - \alpha_1}{|\alpha_1|} e^{-1} < M < \operatorname{ctg}\alpha \left(\frac{\alpha_2 - \alpha_1}{|\alpha_2|} e^{-1} + 2\right) + 1, && \text{for } \alpha_2 \ne \alpha_1 \\ &\operatorname{ctg}\alpha\, e^{\alpha_2 \pi/(\beta_2 - \beta_1)} < M < 2\operatorname{ctg}\alpha + 1, && \text{for } \alpha_2 = \alpha_1 \end{aligned} \tag{7}$$

The proof is in the next section. The estimate (7) involves eigenvalues and angles between eigenvectors, and these parameters sometimes cannot be calculated with acceptable accuracy. The following assertions allow us to replace them with quantities calculated using the matrix spectrum dichotomy method.

First, we present a theorem on estimating angles.

Theorem 2. *Let P and $I - P$ be projections onto invariant subspaces of a matrix. Then the angle between these subspaces satisfies the estimate*

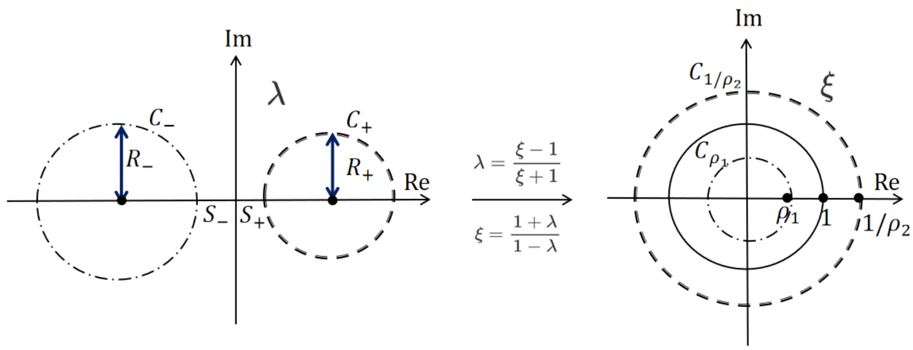

FIG. 8. Scheme of images and prototypes of circles under fractional-linear transformation.

$$\frac{\|P\|^2-1}{2\|P\|} \le \text{ctg}\,\alpha \le \sqrt{\|P\|^2-1}. \tag{8}$$

The proof is given below (section 5).

Note. If eigenvalues are separated using the dichotomy method, then the corresponding eigenvectors are located in different invariant subspaces, and the angle between them will be greater than the angle between the subspaces. Therefore, using the right-hand inequality (8), we can strengthen the upper bound (7). To strengthen the lower bound, the information obtained from a single application of the dichotomy method is insufficient.

Next, we'll consider a method for estimating the real and imaginary parts of eigenvalues. We'll assume that the matrix spectrum is separated relative to a straight line using an algorithm based on a linear-fractional transformation of the complex plane, mapping the imaginary axis to the unit circle (see [14], [15] for more details).

Consider the transformation of the complex plane $\lambda = \frac{\xi-1}{\xi+1}$. In this case, the spectral problem $(A-\lambda I)v = 0$ is transformed into a problem for the matrix pencil $\det((A+I)-\xi(I-A)) = 0$ and the spectral parameter ξ. This fractional-linear transformation maps the imaginary axis in the plane of the parameter λ to the unit circle in the plane of the parameter ξ. Thus, the problem of dichotomy of the spectrum of the matrix A with respect to the imaginary axis is equivalent to the problem of dichotomy of the spectrum of the pencil $A_0 - \xi B_0$ with respect to the unit circle, where $A_0 = A+I$, $B_0 = I - A$. As a criterion for the absence of a spectrum (spectrum dichotomy) of the matrix A on the imaginary axis, the criterion for the absence of a spectrum of the pencil $A_0 - \xi B_0$ on the unit circle can be used:

$$H = \frac{1}{2\pi}\int_0^{2\pi} (A_0 - e^{i\varphi}B_0)^{-*} C (A_0 - e^{i\varphi}B_0)^{-1} d\varphi.$$

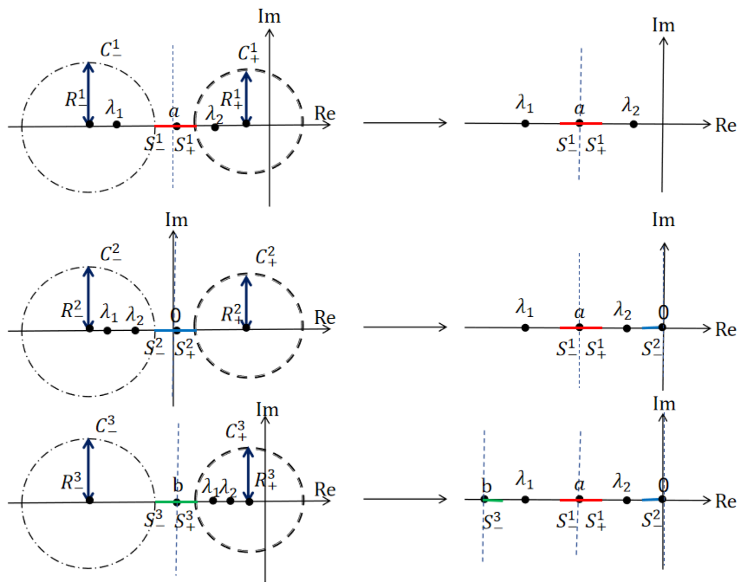

FIG. 9. Scheme for estimating the location of eigenvalues.

If the pencils $A - \lambda B$ and $A_0 - \xi B_0$ have no eigenvalues on the imaginary axis and the unit circle, respectively, then the pencil $A_0 - \xi B_0$ also has no eigenvalues in the annulus between the circles C_{ρ_1} and C_{1/ρ_2} centered at zero and with radii $0 < \rho_1 < 1$ and $1 < 1/\rho_2$ (see Fig. 8), where ρ_1 is the largest modulus of an eigenvalue of the pencil $A_0 - \xi B_0$ that lies inside the unit circle, and $1/\rho_2$ is the smallest modulus of the eigenvalues that lie outside the unit circle. The preimages of these circles are the circles C_- and C_+ lying in the left and right half-planes, respectively. The parameters of these circles are described by the following theorem.

Theorem 3. *For the radii R_-, R_+ of the circles C_-, C_+ and the distances S_-, S_+ from them to the imaginary axis, the estimates are*

$$R_\pm \leq \sqrt{\|H\|^2 - 1},\ S_\pm \geq \|H\| - \sqrt{\|H\|^2 - 1}. \tag{9}$$

The proof is given in the next section.

Note. To perform a dichotomy of the spectrum of a line parallel to the imaginary axis and passing through the point a, we must apply the described approach to the matrix $A - aI$.

This theorem allows us to obtain estimates for the eigenvalues by applying the dichotomy algorithm three or four times. For example, if the eigenvalues $\lambda_{1,2}$ are real (see Theorem 1), then estimates for them can be obtained by applying a dichotomy using three lines: the line separating $\lambda_{1,2}$, the imaginary axis, and the line lying to the left of both eigenvalues, as shown on the scheme 9. Let us consider the dichotomy of the spectrum with respect to the line $x = a$, where $\lambda_1 < a < \lambda_2$, that is, λ_1 is in the circle S^1_- on the left, and λ_2 is inside S^1_+ on the right. In this case, the inequalities will be established

$$S^1_- + S^1_+ \leq \lambda_2 - \lambda_1 \leq S^1_- + S^1_+ + 2(R^1_- + R^1_+),$$
$$a - S^1_- - 2R^1_- \leq \lambda_1 \leq a - S^1_-, \;\; a + S^1_+ \leq \lambda_2 \leq a + S^1_+ + 2R^1_+.$$

The dichotomy with respect to the imaginary axis allows us to obtain estimates

$$\lambda_2 - \lambda_1 \leq 2R^2_-, \;\; -S^2_- - 2R^2_- \leq \lambda_1, \;\; \lambda_2 \leq -S^2_-.$$

And finally, if we perform a dichotomy of the spectrum with respect to the line $x = b$, where $b < \lambda_1 < \lambda_2$, then the following estimates for $\lambda_{1,2}$ will be obtained:

$$\lambda_2 - \lambda_1 \leq 2R^2_+, \;\; b + S^3_+ \leq \lambda_1, \;\; \lambda_2 \leq b + S^3_+ + 2R^2_+.$$

If the imaginary parts of the eigenvalues $\lambda_{1,2}$ are nonzero, then to estimate their difference (see theorem 1), we must perform a dichotomy of the line parallel to the real axis and separating the eigenvalues of interest.

As an example, consider the Cauchy problem $dy/dt = Ay$, $y(0) = y_0$, where

$$A = \begin{bmatrix} 1 & \cos\alpha \\ 0 & \sin\alpha \end{bmatrix} \begin{bmatrix} \lambda_1 & \\ & \lambda_2 \end{bmatrix} \begin{bmatrix} 1 & -\text{ctg}\alpha \\ 0 & \frac{1}{\sin\alpha} \end{bmatrix}, \quad \begin{array}{l} \alpha = 0.01, \\ \lambda_1 = -3, \; \lambda_2 = -2. \end{array} \tag{10}$$

The results of calculations according to the scheme described above are presented in the Table 1. These data allow us to obtain estimates for the eigenvalues

$$-3.0088 < \lambda_1 < -2.9869, \; -2.0294 < \lambda_1 < -1.8481. \tag{11}$$

TABLE 2. Results of applying the dichotomy and theorem 3.

	line $Re\,\lambda = -2.5$	line $Re\,\lambda = 0$	line $Re\,\lambda = -5$
ρ_+	0.3848	0.0545	0.5373
ρ_-	0.3603	0.5023	0.1518
S_+	0.4443	0.8966	0.3010
S_-	0.4703	0.3313	0.7364
R_+	0.9034	0.1093	1.5107
R_-	0.8281	1.3436	0.3108

Also, the dichotomy with respect to the straight line $Re\,\lambda = -2.5$ allows us to obtain estimates for the angle between the eigenvectors:

$$49.9958 \leq \text{ctg}\,\alpha \leq 99.9967. \tag{12}$$

We also use Algorithm 2 to obtain the initial data of the growing solution:

$$y_0 = \begin{bmatrix} -0.00499998 \\ 0.99998750 \end{bmatrix}.$$

Figure 10 shows the norm of the obtained solution, as well as the lines denoting estimates of its maximum. The blue and green lines were obtained

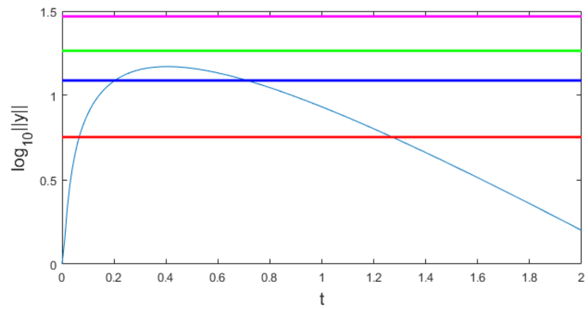

FIG. 10. Comparison of the actual maximum norm of the solution and its estimates

by substituting the known values of $\lambda_{1,2}$ and α (10) into the estimates of the 1 theorem. The red and pink lines denote the estimates that follow from the 1 theorem, but using additional estimates (11), (12).

5 Proofs of Theorems

Proof of Theorem 1.

Let A be an arbitrary diagonalizable matrix. We fix a basis such that the first eigenvector coincides with the first unit vector, and the second eigenvector is decomposed into a linear combination of the first two unit vectors. Then we have the representation $A = T\Lambda T^{-1}$, where

$$T = \begin{bmatrix} 1 & \cos\alpha & * & \cdots & * \\ 0 & \sin\alpha & * & \cdots & * \\ 0 & 0 & * & \cdots & * \\ \vdots & \vdots & \vdots & \vdots & \vdots \\ 0 & 0 & * & \cdots & * \end{bmatrix}, \quad \Lambda = \begin{bmatrix} \lambda_1 & & & & \\ & \lambda_2 & & & \\ & & \lambda_3 & & \\ & & & \ddots & \\ & & & & \lambda_n \end{bmatrix}.$$

Let's consider the Cauchy problem

$$\begin{cases} \dfrac{dy}{dt} = Ay, \\ \\ y|_{t=0} = y_0 \end{cases} \tag{13}$$

and choose the initial data in a special way $y_0 = [y_1^0, y_2^0, 0, \cdots, 0]^T$. Then the solution to the Cauchy problem has the form

$$e^{At}y_0 = \begin{bmatrix} \hat{T}\begin{bmatrix} e^{\lambda_1 t} & 0 \\ 0 & e^{\lambda_2 t} \end{bmatrix} \hat{T}^{-1} \begin{bmatrix} y_1^0 \\ y_2^0 \end{bmatrix} \\ 0 \\ \vdots \\ 0 \end{bmatrix}, \text{ where } \hat{T} = \begin{bmatrix} 1 & \cos\alpha \\ 0 & \sin\alpha \end{bmatrix}.$$

Thus, to study the behavior of the solution of the Cauchy problem (13), it is sufficient to consider its two-dimensional analogue by the matrix

$$\hat{A} = \hat{T}\hat{\Lambda}\hat{T}^{-1}. \qquad (14)$$

Then the matrix exponential is a triangular matrix

$$e^{\hat{A}t} = \begin{bmatrix} 1 & \cos\alpha \\ 0 & \sin\alpha \end{bmatrix} \begin{bmatrix} e^{\lambda_1 t} & \\ & e^{\lambda_2 t} \end{bmatrix} \begin{bmatrix} 1 & -\text{ctg}\alpha \\ 0 & \frac{1}{\sin\alpha} \end{bmatrix} = \begin{bmatrix} e^{\lambda_1 t} & \text{ctg}\alpha(e^{\lambda_2 t} - e^{\lambda_1 t}) \\ 0 & e^{\lambda_2 t} \end{bmatrix},$$

the solution to the Cauchy problem has the form

$$e^{\hat{A}t} \begin{bmatrix} y_1^0 \\ y_2^0 \end{bmatrix} = \begin{bmatrix} e^{\lambda_1 t} y_1^0 + \text{ctg}\alpha(e^{\lambda_2 t} - e^{\lambda_1 t}) y_2^0 \\ e^{\lambda_2 t} y_2^0 \end{bmatrix}$$

and satisfies the estimates

$$|e^{\lambda_1 t} y_1^0 + \text{ctg}\alpha(e^{\lambda_2 t} - e^{\lambda_1 t}) y_2^0| \leq \|y(t)\| \leq |e^{\lambda_1 t} y_1^0 + \text{ctg}\alpha(e^{\lambda_2 t} - e^{\lambda_1 t}) y_2^0| + |e^{\lambda_2 t} y_2^0|.$$

Let us take into account that $\|y_0\| = 1$, $\text{Re}\,\lambda_j < 0$, and set $y_1^0 = 0, y_2^0 = 1$, then

$$|\text{ctg}\alpha(e^{\lambda_2 t} - e^{\lambda_1 t})| \leq \|y(t)\| \leq |\text{ctg}\alpha(e^{\lambda_2 t} - e^{\lambda_1 t})| + 1. \qquad (15)$$

Thus, the local maximum of the solution is formed due to the growth of the function $\text{ctg}\,\alpha|e^{\lambda_2 t} - e^{\lambda_1 t}|$, while the factor $\text{ctg}\alpha$ plays a scaling role. We examine the maximum of the function $E(t, \lambda_1, \lambda_2) = |e^{\lambda_2 t} - e^{\lambda_1 t}|$:

$$E(t, \lambda_1, \lambda_2) = |e^{(\alpha_2 + i\beta_2)t} \pm e^{(\alpha_2 + i\beta_1)t} - e^{(\alpha_1 + i\beta_1)t}|,$$

that is, the growth estimate depends on two different values

$$\check{E} = |e^{(\alpha_2 + i\beta_2)t} - e^{(\alpha_2 + i\beta_1)t}|, \quad \hat{E} = |e^{(\alpha_2 + i\beta_1)t} - e^{(\alpha_1 + i\beta_1)t}|.$$

Note that the point $e^{(\alpha_1 + i\beta_1)t}$ lies on the circle of radius $e^{\alpha_2 t}$, and the points $e^{(\alpha_2 + i\beta_1)t}$ and $e^{(\alpha_2 + i\beta_2)t}$ lie on the circle of radius $e^{\alpha_1 t}$, given that $e^{\alpha_2 t} \geq e^{\alpha_1 t}$. Since $e^{(\alpha_1 + i\beta_1)t}$ and $e^{(\alpha_2 + i\beta_1)t}$ lie on the same radius, and $e^{(\alpha_1 + i\beta_1)t}$ and $e^{(\alpha_2 + i\beta_2)t}$ lie on a chord, the lower bound holds $\hat{E} \leq E$. The upper bound follows from the triangle inequality:

$$\hat{E} \leq E \leq \hat{E} + \check{E}. \qquad (16)$$

Therefore, to estimate E, we need to obtain upper and lower bounds for $\hat{E}$, and upper bounds for $\check{E}$. However, in the exceptional case where $\alpha_1 = \alpha_2$, the equality $E = \check{E}$ holds, so in this situation, a lower bound for $\check{E}$ is required.

We examine $\hat{E}$ and $\check{E}$ separately. The function $\check{E}$ can be transformed as follows.

$$\check{E} = e^{\alpha_2 t} |e^{i(\beta_2 + \beta_1)t/2}| |e^{i(\beta_2 - \beta_1)t/2} - e^{-i(\beta_2 - \beta_1)t/2}| = 2e^{\alpha_2 t} \left| \sin \frac{\beta_2 - \beta_1}{2} t \right|.$$

The upper bound in this case is obvious: $\check{M} < 2$, where $\check{M} = \max \check{E}$. Note that the maximum of the function $\check{E}$ is achieved within the interval

$t \in (0, \pi/(\beta_2 - \beta_1))$, so on its boundary $t = \pi/(\beta_2 - \beta_1)$ the relation $\check{M} \geq 2e^{\alpha_2 \pi/(\beta_2 - \beta_1)}$ is true. As a result, we obtain a two-sided bound

$$2e^{\alpha_2 \pi/(\beta_2 - \beta_1)} \leq \check{M} \leq 2. \tag{17}$$

Let $\hat{M} = \max \hat{E}$. To estimate this value, we transform the function $\hat{E}$ using the mean value theorem

$$\hat{E} = |e^{\alpha_2 t} - e^{\alpha_1 t}| = t\, e^{\xi t} \cdot (\alpha_2 - \alpha_1), \text{ where } \alpha_1 \leq \xi \leq \alpha_2.$$

Then for all $t \geq 0$ the following inequalities hold:

$$(\alpha_2 - \alpha_1)\, t\, e^{\alpha_1 t} \leq \hat{E} \leq (\alpha_2 - \alpha_1)\, t\, e^{\alpha_2 t}.$$

Equating the derivatives of the majorant and minorant with respect to t to zero, we find that they reach their maxima at $t = -\alpha_2^{-1}$ and $t = -\alpha_1^{-1}$, respectively. Substituting these values into their arguments, we obtain the estimates

$$\frac{\alpha_2 - \alpha_1}{|\alpha_1|} e^{-1} \leq \hat{M} \leq \frac{\alpha_2 - \alpha_1}{|\alpha_2|} e^{-1}. \tag{18}$$

Combining the estimates (15), (16), (17), (18), we arrive at the justification of the statement of the theorem 1.

Proof of Theorem 2. Let us prove the left-hand side of the inequality. Let U be the matrix whose columns form an orthogonal basis for the subspace of dimension l that is the image of the transformation P. Similarly, let V be the matrix consisting of orthogonal m basis vectors of the image of the transformation $I_n - P$, $l + m = n$, and I_n the identity matrix of size n. We introduce the matrix $W = [U, V]$. For the projection P, the following representation holds:

$$P = W \begin{pmatrix} I_l & 0 \\ 0 & 0 \end{pmatrix} W^{-1},$$

where I_l is the identity matrix of size l. This implies that $\|P\| \leq \|W\|\, \|W^{-1}\|$. It is known that

$$\sigma_{\max}(W) = \sup_{\|z\|=1} \|Wz\|, \sigma_{\min}(W) = \inf_{\|z\|=1} \|Wz\|.$$

Let us consider the norm $\|Wz\|$ separately and split the vector z into two subvectors: x of size l and y of size m. For them, the following chain of equalities holds:

$$\|Wz\|^2 = \left(W \begin{pmatrix} x \\ y \end{pmatrix}, W \begin{pmatrix} x \\ y \end{pmatrix} \right) =$$
$$= \left([\textstyle\sum_{i=1}^{l} x_i U_i + \sum_{j=1}^{m} y_j V_j] \right), \left([\textstyle\sum_{i=1}^{l} x_i U_i + \sum_{j=1}^{m} y_j V_j] \right) =$$
$$= \textstyle\sum_{i=1}^{l} |x_i^2| + \sum_{m=1}^{j} |y_j^2| + \sum_{i=1}^{l} \sum_{j=1}^{m} (c_{ij} y_j \bar{x_i} + \bar{c_{ij}} x_i \bar{y_j}) =$$
$$= 1 + (Cy, x) + (x, Cy) = 1 + 2Re(Cy, x)$$

where c_{ij} denotes the scalar product (U_i, V_j). Further, we need to find the supremum and infimum of the expression $2Re(Cy, x)$, where $\|x\|^2 + \|y\|^2 = 1$.

We divide C, x, y into real and imaginary parts, where $C = \Theta + i\Omega, x = \alpha + i\beta, y = \xi + i\eta$. Substitute (Cy, x) into the expression

$$(Cy, x) = (\Theta\xi - \Omega\eta + i(\Theta\eta + \Omega\xi), \alpha + i\beta) =$$

$$= (\Theta\xi - \Omega\eta, \alpha) - i(\Theta\xi - \Omega\eta, \beta) + i((\Theta\eta + \Omega\xi), \alpha) + (\Theta\xi + \Omega\xi, \beta)$$

and we get

$$2Re(Cy, x) = 2\left[(\Theta\xi - \Omega\eta, \alpha) + (\Theta\xi + \Omega\xi, \beta)\right].$$

Since $(x, x) = (\alpha, \alpha) + (\beta, \beta)$, $(y, y) = (\xi, \xi) + (\eta, \eta)$, then the Lagrange function for determining the conditional extremum has the form

$$L = 2\left[(\Theta\xi - \Omega\eta, \alpha) + (\Theta\eta + \Omega\xi, \beta)\right] + \sigma\left[(\xi, \xi) + (\eta, \eta) + (\alpha, \alpha) + (\beta, \beta) - 1\right].$$

By equating the expressions for the derivatives to zero, we obtain a system of equalities

$$L_\alpha = 2(Re(Cy + \sigma x)) = 0, \quad L_\beta = 2(Im(Cy + \sigma x)) = 0,$$

$$L_\xi = 2(Re(C^*x + \sigma y)) = 0, \quad L_\eta = 2(Im(C^*x + \sigma y)) = 0.$$

From these it follows that the parameter σ is the singular value of the matrix C, taken with the minus sign, and x and y are the corresponding singular vectors, while

$$(Cy, x) + (C^*x, y) = -\sigma(\|x\|^2 + \|y\|^2) = -\sigma.$$

From this it follows equalities

$$\sup_{\|x\|^2 + \|y\|^2 = 1} [(x, Cy) + (Cy, x)] = \sigma_{\max}(C),$$

$$\inf_{\|x\|^2 + \|y\|^2 = 1} [(x, Cy) + (Cy, x)] = -\sigma_{\max}(C).$$

This means that the following estimates hold for the matrix W

$$(\sigma_{\max} W)^2 = 1 + \sigma_{\max}(C), \quad (\sigma_{\min} W)^2 = 1 - \sigma_{\max}(C).$$

Further, we note that if u and v are some normalized vectors spanned by U_i and V_j, respectively, then

$$1 = \|u\| = \|Ua\| = \|a\|, \qquad 1 = \|v\| = \|Vb\| = \|b\|.$$

Moreover, the cosine of the angle α between the subspaces satisfies the following representation:

$$|\cos\ \alpha| = \max_{\|u\|, \|v\| = 1} |(u, v)| = \max_{\|a\|, \|b\| = 1} |(Ca, b)| = \|C\|,$$

from which it follows that

$$\sigma_{\max}(W) = \sqrt{1 + |\cos\ \alpha|}, \qquad \sigma_{\min}(W) = \sqrt{1 - |\cos\ \alpha|}.$$

Using these equalities leads to an upper bound for the projector norm:

$$\|P\| \le \|W\|\|W^{-1}\| = \frac{\sigma_{\max}(W)}{\sigma_{\min}(W)} = \frac{\sqrt{1 + \cos\alpha}}{\sqrt{1 - \sin\alpha}} = \mathrm{ctg}\frac{\alpha}{2}.$$

Let's consider the formula for the cotangent of a double angle:

$$\operatorname{ctg}\,\alpha = \frac{\operatorname{ctg}^2\frac{\alpha}{2} - 1}{2\operatorname{ctg}\frac{\alpha}{2}}$$

and note the monotonic increase of the function $(x^2 - 1)/x$ for $x > 0$. This implies the inequality

$$\operatorname{ctg}\alpha \geq \frac{\|P\|^2 - 1}{2\|P\|}.$$

Thus, the left-hand side of the inequality is proven.

The proof of the right-hand side of the inequality is as follows. Fix vectors $u = \sum_{i=1}^{l} a_i U_i$ and $v = \sum_{j=1}^{m} b_j V_j$ such that the angle between them is minimal. Among the vectors orthogonal to v, choose a vector x, $\|x\| = 1$, such that the projection of x onto the subspace spanned by the columns of U $Px = cu$ is a vector collinear to u. Vectors u, cv and x form a right triangle such that one leg is vector x, the other leg is directed along vector v, and the hypotenuse is directed along vector u. By the definition of sine, we obtain the equality

$$\sin\alpha = \frac{\|x\|}{\|Px\|} \geq \frac{1}{\|P\|}.$$

Next, we easily obtain

$$\operatorname{ctg}\,\alpha = \frac{\sqrt{1 - \sin^2\alpha}}{\sin\alpha} \leq \sqrt{\|P\|^2 - 1}.$$

Thus, the right-hand side of the inequality is also proven.

Proof of Theorem 3. Consider the circle C_{ρ_1}. Its equation is $\xi\bar{\xi} = \rho_1^2$. It is easy to establish that the equation of its preimage C_- is

$$\lambda\bar{\lambda} - \left(1 - \frac{2}{1 - \rho_1^2}\right)\lambda - \left(1 - \frac{2}{1 - \rho_1^2}\right)\bar{\lambda} + 1 = 0.$$

It follows that the center of this circle is at the real point $O_- = -(1 + \rho_1^2)/(1 - \rho_1^2)$, and the radius is $R_- = 2\rho_1/(1 - \rho_1^2)$. This means that the distance from the circle C_- to the imaginary axis is $S_- = (1 - \rho_1)/(1 + \rho_1)$. Similarly, we obtain $R_+ = 2\rho_2/(1 - \rho_2^2)$ and $S_+ = (1 - \rho_2)/(1 + \rho_2)$. Next, we use the estimate $\rho_{1,2} < \sqrt{\frac{\|H\|-1}{\|H\|+1}}$ [10], which results in the inequalities (9). The theorem is proved.

6 Conclusion

In this paper, for initial-value problems satisfying the spectral stability criterion, a mechanism for the formation of solutions that grow over the initial time interval is revealed. Theorem 1 shows that the initial data of such solutions are special linear combinations of non-orthogonal eigenvectors, with the local maximum of the solution proportional to the cotangent of the angle between them. Theorem 1 also substantiates a two-sided estimate for the maximum value of the solution norm. While the upper bound is, in a sense, a refinement of M.G. Krein's well-known estimate, the lower bound represents a new tool for analyzing ODE systems. The presence of this estimate indicates that the system has a solution that, given normalized initial data, grows beyond a given value. Theorems 2 and 3 allow us to obtain estimates without calculating eigenvalues and eigenvectors, but by applying the matrix spectrum dichotomy method and estimating the positions of the eigenvalues. The angle between the eigenvectors is estimated using the angle between the subspaces in which they lie. This fact suggests that the left-hand side of the inequality (7) can be strengthened in this way only for 2×2 matrices, as shown in the example (10). To correctly strengthen the lower bound for the maximum of solutions in the case of matrices of arbitrary size, it is necessary to use more information about the pseudospectrum spots, which will be the subject of the authors' next paper.

Two algorithms were developed to obtain initial data for locally increasing solutions. Using these algorithms, locally increasing solutions were constructed for two flutter models and a linearized Navier-Stokes system in the neighborhood of plane-parallel Poiseuille flow. It should be noted that the presence of locally increasing solutions in linearized problems may explain so-called «practical» instability.

References

[1] L. N. Trefethen, A. E. Trefethen, S. C. Reddy, T. A. Driscoll, *Hydrodynamic stability without eigenvalues*, Science, **261**:5121 (1993), 578–584. Zbl 1226.76013

[2] M. Buffat, L. L. Penven, *Analysis of transient growth using an orthogonal decomposition of the velocity field in the Orr-Sommerfeld Squire equations*, arXiv preprint, arXiv: 1305.4763 (2013).

[3] S. K. Godunov, *Problem of the dichotomy of the spectrum of a matrix*, Siberian Math. J., **27**:5 (1986), 649–660. Zbl 0655.34020

[4] H. Ya. Bulgakov, S. K. Godunov, *Circular dichotomy of a matrix spectrum*, Siberian Math. J., **29**:5 (1988), 734–744. Zbl 0674.65016

[5] A. N. Malyshev, *Introduction to computational linear algebra*, Nauka, Novosibirsk, 1991 (in russian).

[6] A. N. Malyshev, M. Sadkane, *On parabolic and elliptic spectral dichotomy*, SIAM Journal on Matrix Analysis and Applications, **18**:2 (1997), 265–278. Zbl 0872.65034

[7] S.K. Godunov, M. Sadkane, *Some new algorithms for the spectral dichotomy methods*, Linear Algebra and its Applications, **358** (2003), 173–194. Zbl 1035.65032

[8] S. K. Godunov, M. Sadkane, *Numerical determination of a canonical form of a symplectic matrix*, Siberian Math. J., **42**:4 (2001), 629-647. Zbl 1071.65049

[9] S.K. Godunov, *Modern Aspects of Linear Algebra*, American Mathematical Society, 1998 (in russian).

[10] S.K. Godunov, *Lectures on modern aspects of linear algebra*, Nauka, Novosibirsk, 2002 (in Russian).

[11] V. G. Bunkov, S. K. Godunov, V. B. Kurzin, M. Sadkane, *Application of the new mathematical apparatus "One-dimensional spectral portraits of matrices" to solving the problem of aeroelastic vibrations of blade cascades*, Scientific Notes of TsAGI, **40**:6 (2009), 3-13 (in Russian).

[12] E.A. Biberdorf, M.A. Blinova, N.I. Popova, *Some modifications of the method of matrix spectrum dichotomy and their applications to stability problems*, Numerical Analysis and Applications, **11**:2 (2018), 108-120. Zbl 1413.65090

[13] E.A. Biberdorf, *Development of the matrix spectrum dichotomy method*, Continuum Mechanics, Applied Mathematics and Scientific Computing: Godunov's Legacy: A Liber Amicorum to Professor Godunov. Cham: Springer International Publishing, 2020, 37–43.

[14] E.A. Biberdorf, A.S. Rudometova, L. Wang, A.D. Jumabaev, *A Method for Separating the Matrix Spectrum by a Straight Line and an Infinite Strip Flutter Problem*, Computational Mathematics and Mathematical Physics, **64**:8 (2024), 1704–1714. Zbl 1553.65031

[15] E.A. Biberdorf, L. Wang, *Application of linear fractional transformation in problems of localization of matrix spectra and roots of polynomials*, Sib. Èlektron. Mat. Izv., **21**:2 (2024), 46–63.

[16] S. D. Algasin, I. A. Kiiko, *Flutter of Plates and Shells*, Nauka, Moscow, 2006 (in Russian).

[17] B.V. Semisalov, *A Nonlocal algorithm for solving the Poisson equation and its applications*, Zh. Vychisl. Mat. Mat. Fiz., **54**:7 (2014), 1110-1135 (in Russian).

[18] L. N. Trefethen, *Spectral methods in MATLAB*, PA: SIAM, Philadelphia, 2000. Zbl 0953.68643

[19] G.V. Demidenko, *Matrix equations*, Nauka, Novosibirsk, 2009 (in Russian).

Elina Arnoldovna Biberdorf
Sobolev Institute of Mathematics,
pr. Koptyuga, 4,
630090, Novosibirsk, Russia
Email address: ermolova@math.nsc.ru

Wang Li
Novosibirsk State University,
ul. Pirogova, 1
630090, Novosibirsk, Russia
Email address: l.van3@g.nsu.ru